



Proton-conducting solid oxide fuel cells prepared by a single step co-firing process

Lei Bi, Zetian Tao, Wenping Sun, Shangquan Zhang, Ranran Peng, Wei Liu*

Key Laboratory of Energy Conversion Materials, University of Science and Technology of China and Shanghai Institute of Ceramics, Chinese Academy of Sciences, Hefei, Anhui 230026, People's Republic of China

ARTICLE INFO

Article history:

Received 14 January 2009

Received in revised form 16 February 2009

Accepted 17 February 2009

Available online 3 March 2009

Keywords:

BaCeO₃

Low sintering temperature

Proton conductor

Single step co-firing

Solid oxide fuel cell (SOFC)

ABSTRACT

Proton-conducting solid oxide fuel cells (SOFCs), consisting of BaCe_{0.7}In_{0.3}O_{3-δ} (BCI30)-NiO anode substrates, BCI30 anode functional layers, BCI30 electrolyte membranes and BCI30-LaSr₃Co_{1.5}Fe_{1.5}O_{10-δ} (LSCF) composite cathode layers, were successfully fabricated at 1150 °C, 1250 °C and 1350 °C respectively by a single step co-firing process. The fuel cells were tested with humidified hydrogen (~3%H₂O) as the fuel and static air as the oxidant. The single cell co-fired at 1250 °C showed the highest cell performance. The impedance studies revealed that the co-firing temperature affected the interfacial polarization resistance of a single cell as well as its overall electrolyte resistance.

© 2009 Elsevier B.V. All rights reserved.

1. Introduction

Solid oxide fuel cells (SOFCs) have received considerable attention for their high energy conversion efficiency and low impact to environment as a mean of generating electricity [1,2]. Presently, the developments of SOFCs face some challenges. One of them is the high manufacturing costs, which hinders the commercialization of SOFC [3]. The reduction of the fabrication costs is a main object of current developments in SOFCs. We know that the firing process in the SOFC fabrication consumes much time as well as energy, and multiple firing steps are usually involved for a single cell fabrication [3–6]. Therefore, the reduction of firing steps can greatly reduce the SOFC manufacturing costs. It is well known that the co-firing process can reduce the manufacturing processes. However, up to now, many works in SOFCs are just focused on the co-firing of the bi-layer of substrate and supported electrolyte [7–10]. The co-firing of tri-layer of a single cell, consisting of the support, electrolyte membrane and the electrode, receives much less attention. To realize the co-firing of SOFCs by a single step, it is critical to lower the sintering temperature of the electrolyte materials as the high electrolyte sintering temperature will lead to a severe reaction between electrodes and the electrolyte. Furthermore, the high sintering temperature will also lead to a difficulty in choosing a

substrate material with enough porosity after sintering. Yoon et al. [11–13] have successfully fabricated anode supported SOFCs by a single step co-firing process with scandia-stabilized zirconia and yttrium-stabilized zirconia as the electrolyte materials. Recently, Liu et al. [14] have employed a single step co-firing process to prepare a cathode supported Sm_{0.2}Ce_{0.8}O_{1.9} electrolyte SOFC. These research results indicate that the fabrication of SOFCs by a single step co-firing process is possible and this simple process is quite beneficial to the reduction of manufacturing costs for SOFCs.

The current trend in SOFC developments is the reduction of their working temperatures [14–16]. High temperature proton-conducting oxides, especially the BaCeO₃-based materials, are promising electrolyte candidates for intermediate temperature SOFCs because of their high protonic conductivity and low activation energy [15–18]. However, one of the challenges for the development of proton-conducting SOFCs is the poor sinterability of the BaCeO₃-based materials. The sintering temperature of doped BaCeO₃ is usually higher than 1300 °C [19–21]. Therefore, the multiple firing steps are needed to fabricate a single proton-conducting SOFC. To the best of our knowledge, the fabrication of a proton-conducting SOFC by a single step co-firing process has not been achieved before. In this study, we co-fired the green fuel cells, comprising of the four layers of BaCe_{0.7}In_{0.3}O_{3-δ} (BCI30)-NiO anode substrates, BCI30 anode functional layers, BCI30 electrolyte membranes and BCI30-LaSr₃Co_{1.5}Fe_{1.5}O_{10-δ} (LSCF) composite cathode layers, at different temperatures. The cell performances and the effect of the firing temperature on the polarization resistance as well as the electrolyte resistance were studied.

* Corresponding author. Tel.: +86 551 3606929; fax: +86 551 3601592.
E-mail address: wliu@ustc.edu.cn (W. Liu).

2. Experimental

BaCe_{0.7}In_{0.3}O_{3-δ} (BCI30) powder was synthesized by a modified Pechini method. Ba(NO₃)₂, Ce(NO₃)₃·6H₂O and In(NO₃)₃ were dissolved at the stoichiometric ratio and citric acid was then added, which was used as complexation agent. Molar ratio of citric acid/metal set at 1.5. The solution was heated under stirring to evaporate water until it changed into viscous gel and finally ignited to flame, resulting in a white ash. The ash was calcined at 1000 °C for 6 h to form fine BCI30 powders. The BCI30 powder was well mixed with NiO in a weight ratio of 40:60 as the anode. To form sufficient porosity in the anode, 10 wt.% starch was added as the pore former. The BCI30 anode functional powder was prepared by mixing the BCI30 powder and NiO in a weight ratio of 50:50. BCI30 anode functional layers and BCI30 membranes were fabricated on NiO-BCI30 anode substrates by a co-pressing method and the thickness of the layers was controlled by varying the amounts of the powders used. The mixed BCI30 and NiO anode powder was pressed under 200 MPa as green substrates with 15 mm in diameter and 0.6 mm in thickness. The anode functional layer powder and the substrate were co-pressed at 250 MPa to form a green bi-layer of the anode substrate and the anode functional layer. Then the BCI30 powder was co-pressed with the above green bi-layer at 300 MPa to form a green tri-layer structure of a BCI30-NiO anode substrate, a BCI30 anode functional layer, a BCI30 electrolyte layer. A cathode slurry, consisting of BCI30 and LaSr₃Co_{1.5}Fe_{1.5}O_{10-δ} (LSCF) powders (weight ratio of 30:70) and ethyl cellulose-terpineol vehicle, was printed on surface of the electrolyte. Finally, the green single cells, consisting of BaCe_{0.7}In_{0.3}O_{3-δ} (BCI30)-NiO anode substrates, BCI30 anode functional layers, BCI30 electrolyte membranes and BCI30-LaSr₃Co_{1.5}Fe_{1.5}O_{10-δ} (LSCF) composite cathode layers, were co-fired at 1150 °C, 1250 °C and 1350 °C for 5 h respectively to form single cells.

Powder X-ray diffraction (XRD) measurements were made using a Philips X'Pert Pro Super diffractometer with CuKα radiation. Electrochemical measurements of the fuel cell were performed in an Al₂O₃ test housing placed inside a furnace. Humidified hydrogen (~3% H₂O) was fed to the anode chamber at a flow rate of 25 mL min⁻¹, while the cathode was exposed to atmospheric air. The anode side was sealed with Ag paste. Two silver wires were connected to each electrode as current leads. Fuel cell performances were measured with DC Electronic Load (ITech Electronics model IT8511). Resistances of the cells under open circuit condition were measured at different temperatures by an impedance analyzer (CHI604C, Chenhua Inc., Shanghai). A 5 mV a.c. signal was applied and the frequency was swept from 100 KHz to 0.1 Hz. A scanning electron microscope (SEM, JEOL JSM-6700F) was employed to observe the fracture morphology of the assembled single cells and the surface of the cathode layers after firing.

3. Results and discussion

The phase of the as-prepared BCI30 powder was examined with X-ray diffraction. Fig. 1 presents the XRD spectra of BCI30 powder after firing at 1000 °C for 6 h. It can be seen that there are only peaks corresponding to BCI30, without any formation of other substance.

Fig. 2 presents the SEM images of the single cells co-fired at different temperatures. The cells, which were co-fired at 1150 °C, 1250 °C and 1350 °C, were named as Cell-1150, Cell-1250 and Cell-1350 respectively for short. Each SEM image presents a four-layer structure with a porous anode substrate, an anode functional layer, a dense electrolyte membrane and a porous cathode. We can see that the BCI30 membranes are dense, which implies the BCI30 electrolyte membrane became dense even after firing at 1150 °C, much lower than the sintering temperature for the other doped BaCeO₃ materials. The dense BCI30 membranes are about 20 μm in

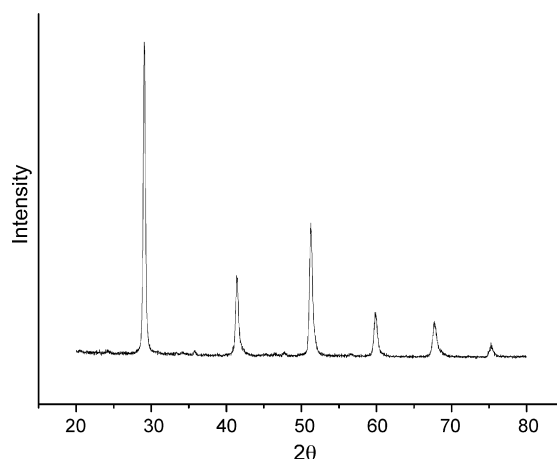


Fig. 1. XRD spectra of BCI30 powder after calcining at 1000 °C for 6 h.

thickness. We also note that with the increasing co-firing temperature, the microstructure of the cathode layer of the cells became less porous, which may block the transportation of the air at the cathode side. Fig. 3 also shows top views of the cathode layers of the single cells co-fired at 1150 °C, 1250 °C and 1350 °C, respectively. The cathode particle size increased gradually with the higher co-firing temperatures. This result implies that the length of triple-phase boundary (TPB), where electrochemical reactions take place, becomes smaller with the increase of co-firing temperatures [22]. Therefore, it is expected that the Cell-1150 can achieve the highest cell performance as it shows the best cathode microstructure, which will lead to a lower polarization loss. Furthermore, with the lower co-firing temperature, the reaction between the cathode and the electrolyte became less severe [23].

For the preliminary fuel cell testing, we used the LaSr₃Co_{1.5}Fe_{1.5}O_{10-δ} (LSCF)-BCI30 composite material as the cathode, in which LSCF has been proven to be a good cathode material for oxygen-ion SOFCs [24]. Shown in Fig. 4 are the *I*-*V* and power density curves of the Cell-1150, Cell-1250 and Cell-1350 at 700 °C. With humidified hydrogen (~3% H₂O) as the fuel, the open circuit voltages (OCV) are 0.936, 0.905 and 0.903 V for the Cell-1150, Cell-1250 and Cell-1350 respectively, which agrees with the SEM results that the BCI30 electrolyte membranes fired at different temperatures are quite dense, as any leakage of gas will lead to severe OCV drops. It has to be mentioned that the Cell-1150 has the highest OCV value though it was fired at the lowest temperature. The highest OCV value for the Cell-1150 may be due to the higher oxygen partial pressure at the cathode side. As we used a single step co-firing process to prepare the cells, the cathode was co-fired together with the electrolyte at different temperatures. We know that the higher co-firing temperature will lead to a lower cathode porosity, which will partially block the oxygen diffusion at the cathode side, especially the static air in our experimental condition. The cathode of the Cell-1150 was fired at the lowest temperature, which led to a more porous cathode layer. The more porous cathode microstructure can lead to the easier diffusion of oxygen to the cathode catalyst layer, thus resulting in a higher oxygen partial pressure at the cathode side for the cell co-fired at a lower temperature. The OCV of the fuel cell is considered proportional to the oxygen partial pressure, so the higher oxygen partial pressure at the cathode side for the Cell-1150 gives rise to a positive spike in cell voltage. The maximum power densities of 114, 160, 63 mW cm⁻² were obtained for the Cell-1150, Cell-1250 and Cell-1350 respectively at 700 °C. The Cell-1250, not the Cell-1150 as we expected, shows the highest cell performance. There must be other factors besides the cathode microstructure governing the cell performance.

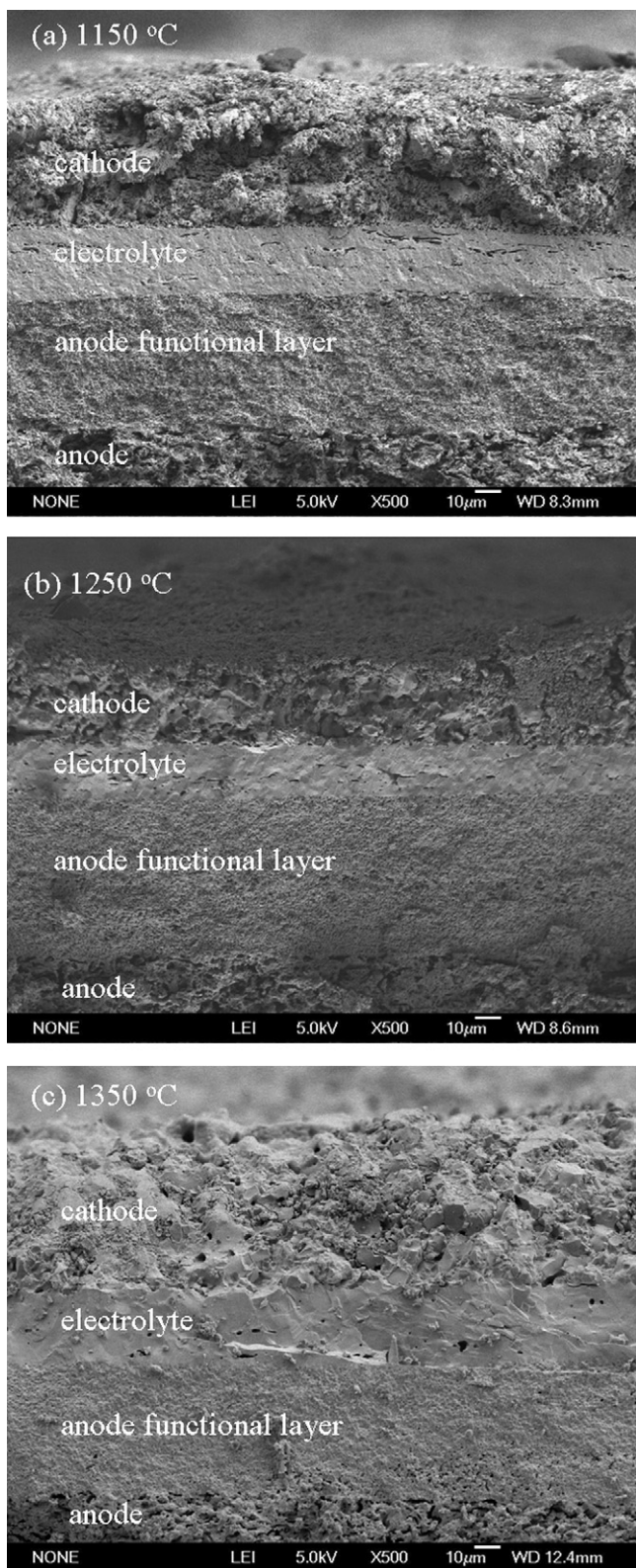


Fig. 2. Cross-section views of the four-layer green cells fired at (a) 1150 °C, (b) 1250 °C and (c) 1350 °C.

Resistances of the single cells under open circuit conditions were investigated by AC impedance spectroscopy. Three typical impedance spectra for Cell-1150, Cell-1250 and Cell-1350, measured at 700 °C, are shown in Fig. 5. The intercept with the real axis at high frequencies represents the ohmic resistance of the

cell including ionic resistance of the electrolyte and some contact resistance associated with interfaces, which is usually taken as the overall electrolyte resistance of the cell. The low frequency intercept corresponds to the total resistance of the cell. Therefore, the difference between the high frequency and low frequency intercepts with

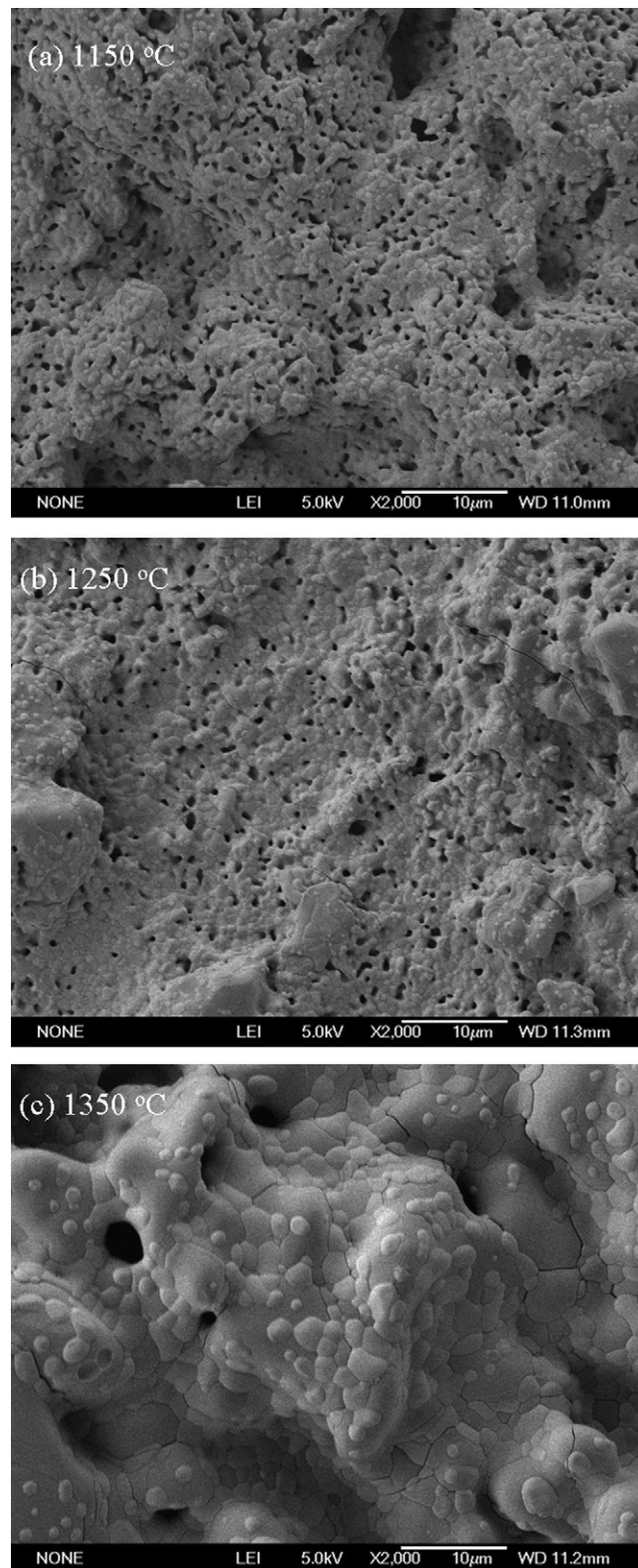


Fig. 3. SEM images of top views of the cathode layers fired at (a) 1150 °C, (b) 1250 °C and (c) 1350 °C.

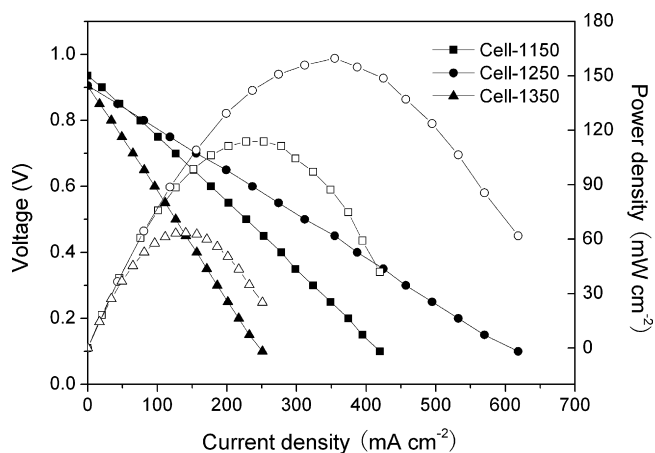


Fig. 4. Performances of different temperature co-fired BCI30-based single cells with humidified hydrogen at 700 °C.

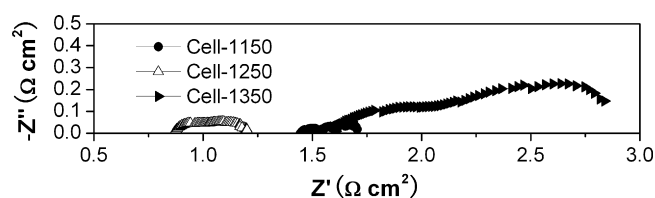


Fig. 5. Impedance spectra of different temperature co-fired single cells measured at 700 °C.

the real axis represents the total interfacial polarization resistance (R_p) of the cell. Fig. 6 presents the total cell resistances, the overall electrolyte resistances and R_p of the cells as determined from the impedance spectra at 700 °C. The overall electrolyte resistances of the cells are 1.45, 0.86 and 1.6 $\Omega \text{ cm}^2$ for the Cell-1150, Cell-1250 and Cell-1350 respectively. The R_p values for the Cell-1150, Cell-1250 and Cell-1350 are 0.25, 0.33 and 1.23 $\Omega \text{ cm}^2$. The impedance analysis shows that the R_p becomes greater with the increase of the firing temperature. This result shows agreement with our expectation that the higher temperature fired cathode layer leads to a smaller TPB and a greater polarization resistance, as we discussed above. It is noted that the Cell-1250 shows the smallest overall electrolyte resistance. It seems when a single green cell was co-fired at 1250 °C, the electrolyte layer and the cathode layer had a better connection than the single cell fired at 1150 °C, but the higher

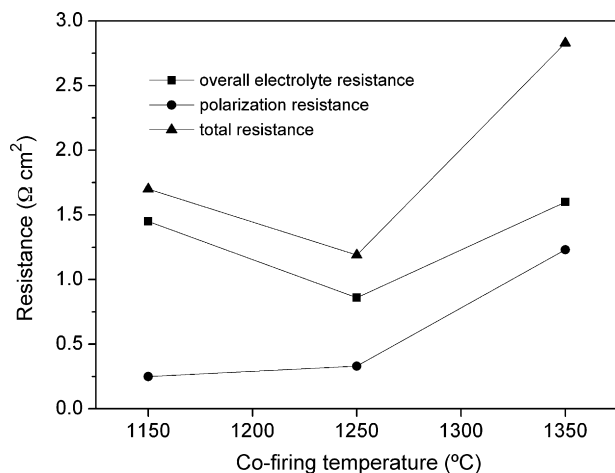


Fig. 6. Total resistance, overall electrolyte resistance and interfacial polarization resistance of the fuel cells as a function of co-firing temperature measured at 700 °C.

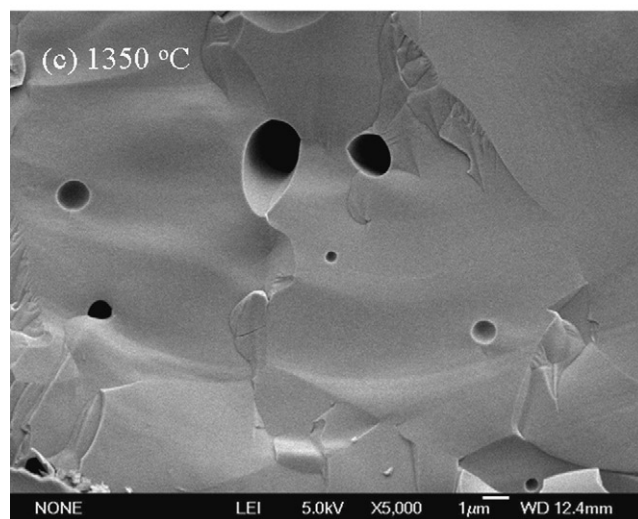
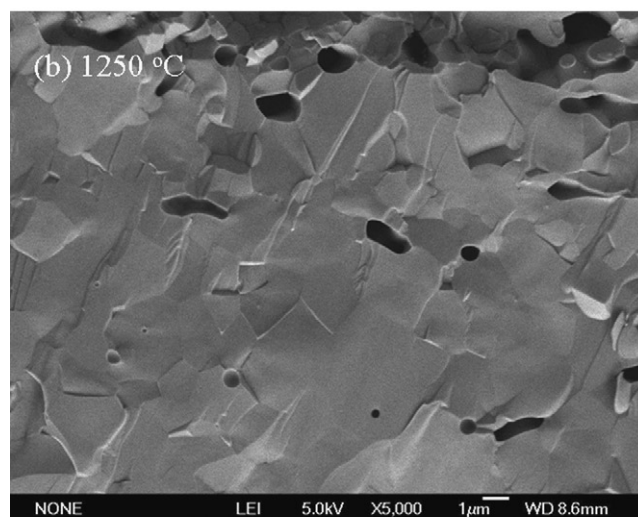
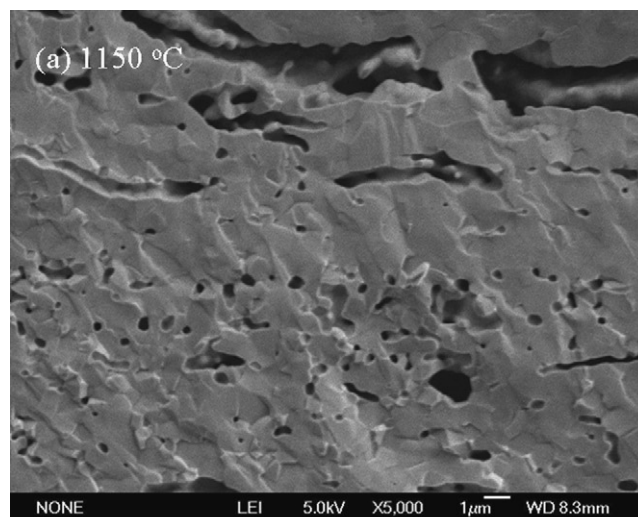


Fig. 7. SEM images of the electrolyte membranes fired at (a) 1150 °C, (b) 1250 °C and (c) 1350 °C.

sintering temperature of 1350 °C led to a severer reaction between the electrolyte layer and the cathode layer, which increased the contact resistance [23]. However, Fig. 7 shows the SEM images of the electrolyte for the Cell-1150, Cell-1250 and Cell-1350 after firing. We can see that with the increasing firing temperature, the

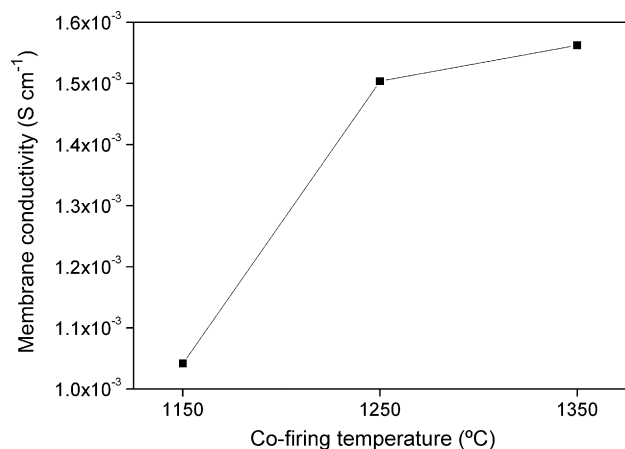


Fig. 8. The electrical conductivity of the BCI30 membrane as a function of co-firing temperature measured at 700 °C.

BCI30 electrolyte membrane became denser. Although the electrolyte membrane of the Cell-1150 is gastight, many close pores exist in the electrolyte, which may decrease the electrolyte conductivity. The differences in the overall electrolyte resistance for these cells may partially result from the different densification of the membranes fired at different temperatures. Therefore, the differences in the overall electrolyte resistance for these cells cannot just be explained by the different contact resistance.

In order to prove this point, we tested the conductivities of the supported BCI30 membranes by a.c. impedance. The anode supported BCI30 membranes were fired at 1150 °C, 1250 °C and 1350 °C respectively to form half-cells with the structure of BCI30 membranes on BCI30-NiO anode substrates. Then Pt paste was printed on these BCI30 membranes and then fired at 900 °C for 1 h. As shown in Fig. 8, the BCI30 membrane fired at 1150 °C shows the lowest electrical conductivity, which agrees with the SEM result shown in Fig. 7(a) that the close pores decrease the electrical performance of the BCI30 membrane greatly. The conductivity of a BCI30 membrane shows a dramatic increase when the membrane was fired at 1250 °C. The Fig. 7(a and b) indicates that the BCI30 membrane fired at 1250 °C shows a higher density compared to the BCI30 membrane fired at 1150 °C, which is beneficial to the enhancement of the electrical conductivity. When the firing temperature further increases to 1350 °C, the conductivity of the BCI30 membrane shows only a slight increase compared to the BCI30 membrane fired at 1250 °C, which implies the higher temperatures only affect the membrane conductivities a little. The Fig. 7(b and c) also reveals that the densification of the BCI30 membranes shows no significant change when the firing temperature increased from 1250 °C to 1350 °C. From the above discussion, we know that although the single cell co-fired at 1150 °C shows the lowest polarization resistance, the low membrane conductivity of the membrane fired at 1150 °C limits its application in SOFC. In another aspect, the single cell co-fired at 1350 °C shows a too high polarization resistance regardless its highest membrane conductivity, which results in the poorest cell performance among these three single cells. The firing temperature of 1250 °C seems to be an optimized fabrication condition for

a BCI30-based proton-conducting SOFC prepared by a single step co-firing process, which achieve high membrane conductivity as well as a reasonable polarization resistance. As a result, the cell co-fired at 1250 °C shows the lowest total cell resistance and the best single cell performance. Considering its single step co-firing process, it makes this type of BCI30-based proton-conducting SOFC interesting for manufacture.

4. Conclusions

A single step co-firing process was successfully employed to fabricate BCI30-based proton-conducting SOFCs. The four-layer green SOFCs, consisting of anode substrates, anode functional layers, electrolyte membranes and cathode layers, were co-fired at 1150 °C, 1250 °C and 1350 °C respectively to form single cells. The supported BCI30 membranes became gastight after firing at these temperatures. Although the cell co-fired at 1150 °C showed the lowest polarization resistance and the cell co-fired at 1350 °C showed the highest membrane conductivity, the cell co-fired at 1250 °C seems to reach a proper compromise between the polarization resistance and the membrane conductivity, which led to the lowest total cell resistance and the best cell performance of these single cells.

Acknowledgements

This work is supported by the Key Program of Chinese Academy of Sciences (Grant No.: KJCX1.YW07) and the National Natural Science Foundation of China (Grant No.: 50730002).

References

- [1] D.J.L. Brett, A. Atkinson, N.P. Brandon, S.J. Skinner, *Chem. Soc. Rev.* 37 (2008) 1568.
- [2] P. Holtappels, U. Vogt, T. Graule, *Adv. Eng. Mater.* 7 (2005) 292.
- [3] L.C. De Jonghe, C.P. Jacobson, S.J. Visco, *Annu. Rev. Mater. Res.* 33 (2003) 169.
- [4] L. Bi, S.Q. Zhang, S.M. Fang, L. Zhang, K. Xie, C.R. Xia, W. Liu, *Electrochem. Commun.* 10 (2008) 1005.
- [5] W.A. Meulenbergh, J.M. Serra, T. Schober, *Solid State Ionics* 177 (2006) 2851.
- [6] J.M. Serra, W.A. Meulenbergh, *J. Am. Ceram. Soc.* 90 (2007) 2082.
- [7] J.M. Serra, O. Buchler, W.A. Meulenbergh, H.P. Buchkremer, *J. Electrochem. Soc.* 154 (2007) B334.
- [8] Z.P. Shao, S.M. Haile, *Nature* 431 (2004) 170.
- [9] L. Bi, S.Q. Zhang, S.M. Fang, Z.T. Tao, R.R. Peng, W. Liu, *Electrochem. Commun.* 10 (2008) 1598.
- [10] L. Bi, S.Q. Zhang, S.M. Fang, L. Zhang, H.Y. Gao, G.Y. Meng, W. Liu, *J. Am. Ceram. Soc.* 91 (2008) 3806.
- [11] K.J. Yoon, W.H. Huang, G.S. Ye, S. Gopalan, U.B. Pal, D.A. Seccombe, *J. Electrochem. Soc.* 154 (2007) B389.
- [12] K.J. Yoon, P. Zink, S. Gopalan, U.B. Pal, *J. Power Sources* 172 (2007) 39.
- [13] P.A. Zink, K.J. Yoon, W.H. Huang, S. Gopalan, U.B. Pal, D.A. Seccombe, *Mater. Res. Soc. Symp. Proc.* 972 (2007) 199.
- [14] M.F. Liu, D.H. Dong, F. Zhao, J.F. Gao, D. Ding, X.Q. Liu, G.Y. Meng, *J. Power Sources* 182 (2008) 585.
- [15] K.D. Kreuer, *Annu. Rev. Mater. Res.* 33 (2003) 333.
- [16] A. D'Epifani, E. Fabbri, E. Di Bartolomeo, S. Licocchia, E. Traversa, *Fuel Cells* 8 (2008) 69.
- [17] N. Maffei, L. Pelletier, J.P. Charland, A. McFarlan, *Fuel Cells* 7 (2007) 323.
- [18] F. Giannici, A. Longo, A. Balerna, K.D. Kreuer, A. Martorana, *Chem. Mater.* 19 (2007) 5714.
- [19] M. Asamoto, H. Shirai, H. Yamaura, H. Yahiro, *J. Eur. Ceram. Soc.* 27 (2007) 4229.
- [20] Z.M. Zhong, *Solid State Ionics* 178 (2007) 213.
- [21] N. Maffei, L. Pelletier, J.P. Charland, A. McFarlan, *J. Power Sources* 140 (2005) 264.
- [22] H. Yamaura, T. Ikuta, H. Yahiro, G. Okada, *Solid State Ionics* 176 (2005) 269.
- [23] L. Yang, C.D. Zuo, S.Z. Wang, Z. Cheng, M.L. Liu, *Adv. Mater.* 20 (2008) 3280.
- [24] K.T. Lee, A. Manthiram, *Chem. Mater.* 18 (2006) 1621.